Uncertainty Quantification of Quarkonium and Heavy Flavor Production

R. Vogt

Lawrence Livermore National Laboratory, Livermore, CA 94551, USA

Physics Department, University of California, Davis, CA 95616, USA

Motivation

- Charm production on edge of perturbative calculations, uncertainties can be large (as will be shown)
- Charmonium (J/ψ, ψ', χ_c) production in color evaporation model uses same parameter set as total charm production
- Defining realistic uncertainty on charmonium cross section requires a better estimate of the total charm cross section
- First attempt to describe total cross section data involved using same parameters as FONLL approach to p_T distributions
  - None of the parameter sets describe total cross section data well
  - Uncertainties too broad to be at all predictive
- Make χ^2 fit to production cross section data
  - Use charm mass from Particle Data Group evaluation
  - Scale uncertainties obtained from map of χ^2 surface
  - Use results in calculation of J/ψ uncertainty, check how previous results, including cold matter effects, change with new parameter set

Sources of Theoretical Uncertainty

Three main sources, all intertwined:

Mass: $1.3 < m < 1.7$ **GeV for charm (central value, 1.5 GeV);** *lattice calculations of charm quark mass suggest lower mass,* 1.27 ± 0.09 *GeV, as do earlier, by eye fits*

Scale: renormalization, μ_R**, and factorization,** μ_F**, scales governing** α_s **and PDF behavior respectively**

Parton Density: use CT10 $\mu_{\rm min} = 1.3$ **GeV,** $\Lambda_{\rm QCD}^{n_f=5} = 0.226$ **GeV**

Setting Limits on the Theoretical Uncertainty

Typical method used for FONLL at RHIC and Tevatron energies

With a given PDF set define a fiducial region of mass and scale that should encompass the true value:

- **For $\mu_F = \mu_R = m$, vary mass between upper and lower end of range;**
- **For central mass value, vary scales independently within a factor of two: $(\mu_F/m, \mu_R/m) = (1,1)$, (2,2), (0.5,0.5), (0.5,1), (1,0.5), (1,2), (2,1).**

Define upper and lower bounds of theoretical values; the maximum and minimum may not come from the same set of parameters at a given energy or p_T

The uncertainty band comes from the upper and lower limits of mass and scale uncertainties added in quadrature:

$$\sigma_{\rm max} = \sigma_{\rm cent} + \sqrt{(\sigma_{\mu,\rm max} - \sigma_{\rm cent})^2 + (\sigma_{m,\rm max} - \sigma_{\rm cent})^2}$$

$$\sigma_{\rm min} = \sigma_{\rm cent} - \sqrt{(\sigma_{\mu,\rm min} - \sigma_{\rm cent})^2 + (\sigma_{m,\rm min} - \sigma_{\rm cent})^2}$$

Large Uncertainty Due to Scale Choice

Large values of α_s for renormalization scales below charm quark mass, m, leads to nonconvergence of perturbative expansion

Convergence improves for larger scales and also for other PDFs with lower initial scales and values of $\Lambda_{\rm QCD}$

Backwards evolution required for low scale ($\mu_F/m = 0.5,\ 1$) charm production

At $x < 0.01$, the CT10 gluon distribution with $\mu_F/m = 0.5$ turns over while $\mu_F/m = 1$ is almost independent of x; less difference between higher scales

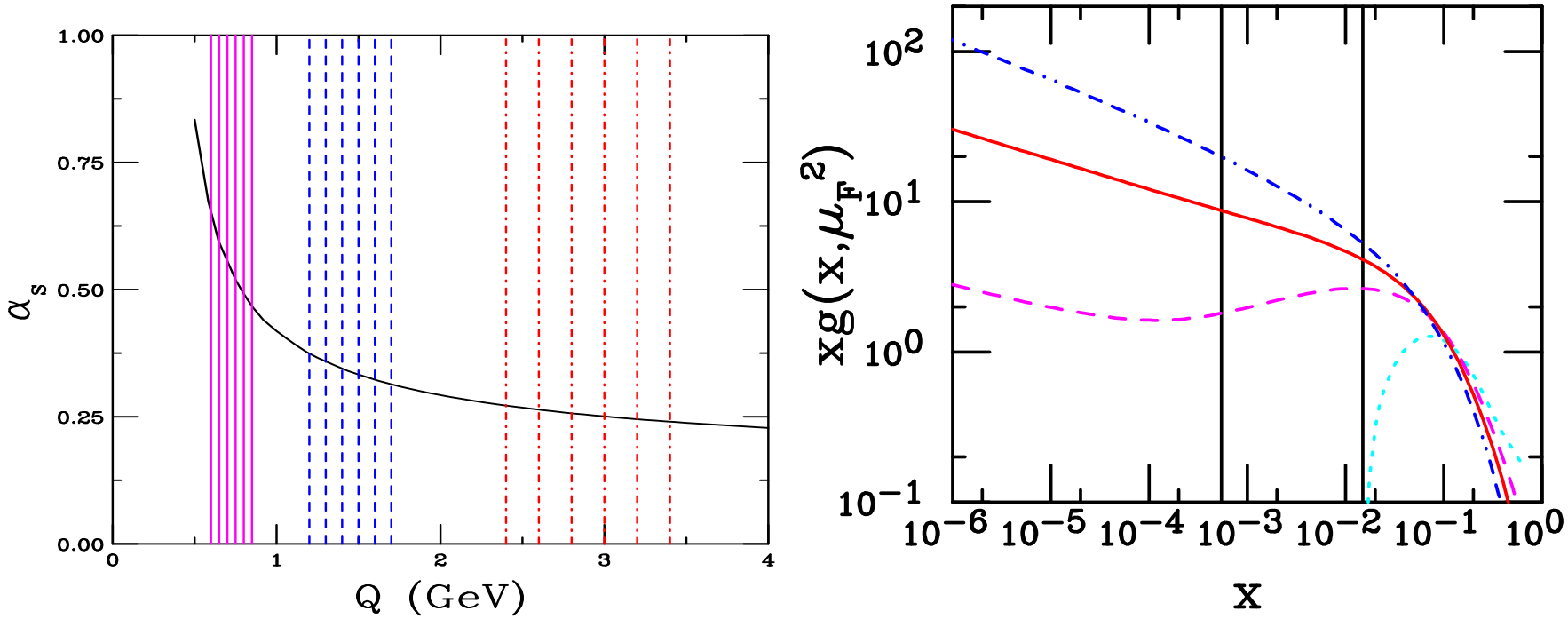

Figure 1: **(Left) The running coupling constant for CT10 with $\Lambda^{n_f=5} = 0.226$ GeV. The vertical bars are clustered around $\mu_R = m/2$, m and $2m$ for $1.2 < m < 1.7$ GeV. (Right) The CT10 gluon distributions as a function of x for $\mu_F/m = 0.5$ (dot-dashed), 1 (dashed), 2 (solid) and 6 (dot-dot-dash-dash-dashed) for $m = 1.5$ GeV. The vertical lines are at $x = 2m/\sqrt{S}$ with $\sqrt{S} = 200$ GeV and 5.5 TeV.**

$c\bar{c}$ Uncertainty with FONLL Fiducial Sets

$c\bar{c}$ cross section dependence on $\sqrt{s}$ with FONLL parameter sets (left), uncertainty band on $c\bar{c}$ cross section (right)

None of the FONLL sets fit the data, large χ^2/dof

No convergence for $\mu_R/m < 1$ (large α_s)

Problems with backward evolution of PDFs for $\mu_F/m \leq 1$ (near or below minimum scale of PDFs)

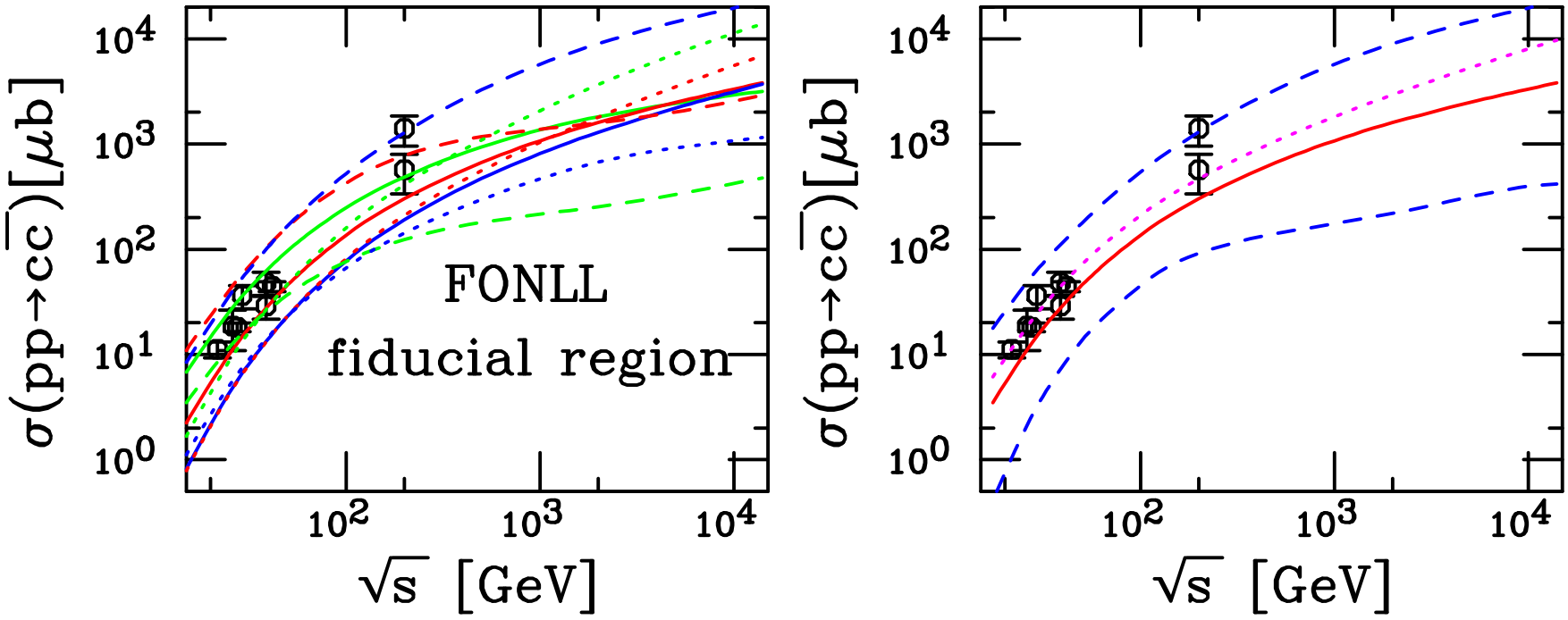

Figure 2: **(Left) Total $c\bar{c}$ cross sections calculated using CTEQ6M. The solid red curve is the central value $(m, \mu_F/m, \mu_R/m) = (1.5\,\mathrm{GeV}, 1, 1)$. The green and blue solid curves are $(1.3\,\mathrm{GeV}, 1, 1)$ and $(1.7\,\mathrm{GeV}, 1, 1)$ respectively. The red, blue and green dashed curves correspond to $(1.5\,\mathrm{GeV}, 0.5, 0.5)$, $(1.5\,\mathrm{GeV}, 1, 0.5)$ and $(1.5\,\mathrm{GeV}, 0.5, 1)$ while the red, blue and green dotted curves are for $(1.5\,\mathrm{GeV}, 2, 2)$, $(1.5\,\mathrm{GeV}, 1, 2)$ and $(1.5\,\mathrm{GeV}, 2, 1)$. (Right) Uncertainty band formed from adding mass and scale uncertainties in quadrature.**

What is the *Best* Fit on Which to Base an Uncertainty?

None of the FONLL fiducial sets gives a good fit to the data

Several similar quality fits to smaller subset of data

What is 'central' result and how to set limits on the uncertainty?

Preferably exclude results with $\mu_R/m < 1$ where α_s is large and $\mu_F/m < 1$ where factorization scale close to initial scale of PDF evolution

Make grid of m, μ_F/m and μ_R/m for $1 \leq m \leq 1.6$ GeV, $0.5 \leq \mu_F/m \leq 7$, $0.5 \leq \mu_R/m \leq 3$

Extract the uncertainty on the scales using PDG mass ($m = 1.27 \pm 0.09$ GeV) for central mass value by determining the farthest extent of the $\Delta\chi^2 = 1.0$ contour (assuming errors follow normal distribution), with Tony Frawley

Check the robustness and energy dependence of the results

Fit Results for Various Cases, Masses

	STAR and PHENIX			PHENIX, no STAR			fixed-target only		
m (GeV)	μ_F/m	μ_R/m	χ^2/dof	μ_F/m	μ_R/m	χ^2/dof	μ_F/m	μ_R/m	χ^2/dof
1.21	$3.4^{+3.60}_{-1.81}$	$2.0^{+0.22}_{-0.18}$	1.51	$2.0^{+1.80}_{-0.87}$	$2.1^{+0.21}_{-0.13}$	1.01	$1.3^{+1.31}_{-0.59}$	$2.2^{+0.16}_{-0.16}$	1.02
1.24	$2.6^{+3.96}_{-1.11}$	$1.8^{+0.13}_{-0.18}$	1.52	$1.8^{+1.61}_{-0.68}$	$1.9^{+0.15}_{-0.12}$	1.01	$1.2^{+1.14}_{-0.47}$	$1.9^{+0.14}_{-0.12}$	1.02
1.27	$2.8^{+3.11}_{-1.39}$	$1.6^{+0.15}_{-0.11}$	1.53	$1.5^{+1.55}_{-0.51}$	$1.6^{+0.10}_{-0.13}$	1.02	$1.1^{+1.00}_{-0.40}$	$1.6^{+0.13}_{-0.08}$	1.03
1.30	$2.2^{+2.98}_{-0.96}$	$1.4^{+0.10}_{-0.10}$	1.53	$1.4^{+1.34}_{-0.52}$	$1.4^{+0.09}_{-0.09}$	1.02	$1.0^{+0.99}_{-0.49}$	$1.5^{+0.07}_{-0.11}$	1.03
1.33	$2.0^{+2.37}_{-0.90}$	$1.2^{+0.09}_{-0.07}$	1.54	$1.3^{+1.19}_{-0.46}$	$1.3^{+0.07}_{-0.08}$	1.02	$1.0^{+0.75}_{-0.36}$	$1.3^{+0.10}_{-0.05}$	1.03
1.36	$1.6^{+2.35}_{-0.60}$	$1.1^{+0.05}_{-0.08}$	1.56	$1.2^{+1.04}_{-0.46}$	$1.1^{+0.08}_{-0.05}$	1.02	$0.9^{+0.72}_{-0.30}$	$1.2^{+0.05}_{-0.08}$	1.04
1.39	$1.4^{+2.24}_{-0.50}$	$1.1^{+0.04}_{-0.08}$	1.57	$1.1^{+0.86}_{-0.42}$	$1.1^{+0.06}_{-0.05}$	1.03	$0.8^{+0.70}_{-0.44}$	$1.1^{+0.08}_{-0.03}$	1.05
1.42	$1.4^{+1.78}_{-0.46}$	$0.9^{+0.04}_{-0.06}$	1.56	$1.1^{+0.82}_{-0.38}$	$0.9^{+0.06}_{-0.04}$	1.03	$0.8^{+0.70}_{-0.68}$	$0.9^{+0.08}_{-0.03}$	1.08
1.45	$1.4^{+1.33}_{-0.63}$	$0.8^{+0.05}_{-0.03}$	1.56	$0.8^{+1.05}_{-0.26}$	$0.9^{+0.03}_{-0.07}$	1.08	$0.7^{+0.56}_{-0.27}$	$0.9^{+0.03}_{-0.05}$	1.03
1.48	$1.1^{+1.31}_{-0.40}$	$0.8^{+0.03}_{-0.04}$	1.56	$0.9^{+0.74}_{-0.33}$	$0.8^{+0.04}_{-0.03}$	1.04	$0.7^{+0.57}_{-0.26}$	$0.8^{+0.06}_{-0.02}$	1.09
1.51	$0.9^{+1.66}_{-0.29}$	$0.8^{+0.02}_{-0.05}$	1.59	$0.8^{+0.61}_{-0.29}$	$0.8^{+0.03}_{-0.03}$	1.04	$0.6^{+0.48}_{-0.15}$	$0.8^{+0.04}_{-0.02}$	1.03
1.54	$0.9^{+1.66}_{-0.33}$	$0.7^{+0.02}_{-0.05}$	1.61	$0.7^{+0.62}_{-0.24}$	$0.7^{+0.02}_{-0.04}$	1.05	$0.6^{+0.33}_{-0.10}$	$0.7^{+0.03}_{-0.02}$	1.03

Results of Contour Extraction for $m = 1.27$ GeV

Results shown for fits with more to less data included

Including more RHIC data broadens the mu_F/m range inside $\Delta\chi^2 = 1$ contour and moves central value toward relatively high μ_F/m (larger than 2)

Including STAR point gives significantly larger χ^2

Value and uncertainty of μ_R/m is not strongly affected by number of data points included in fit

Higher masses narrow contour in both directions and require $\mu_F/m < 1$

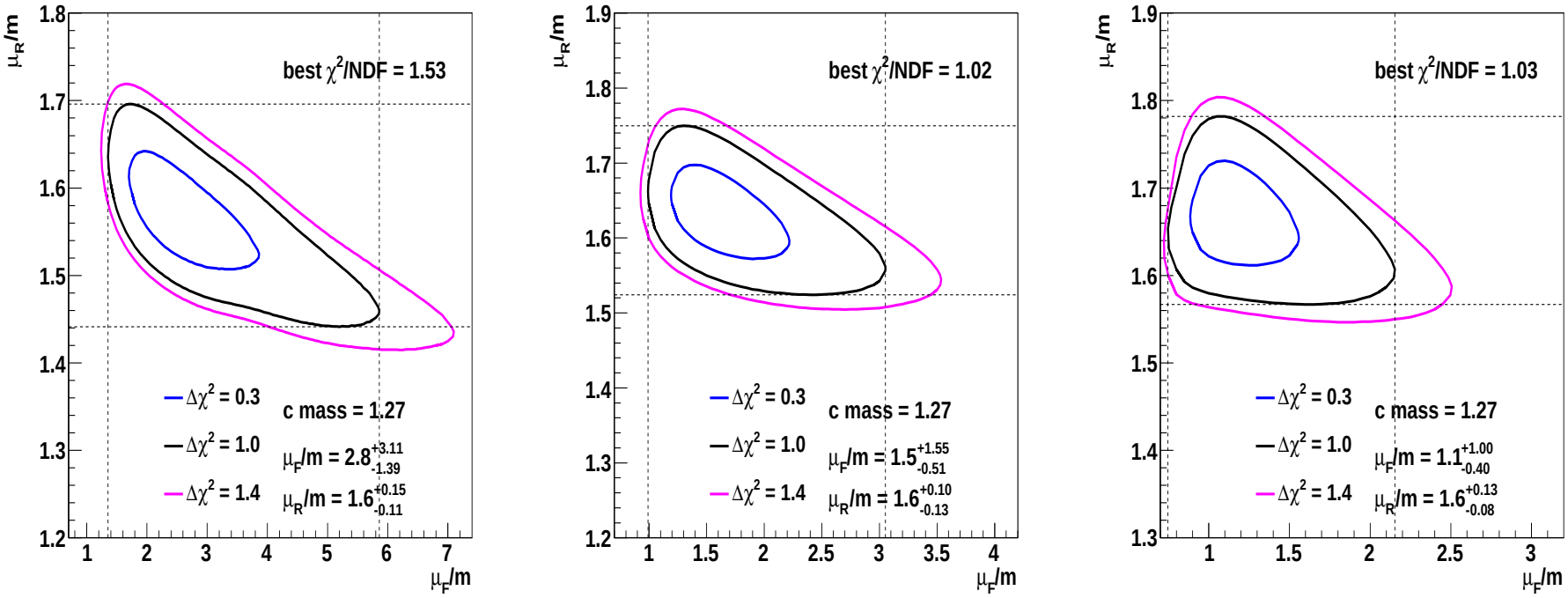

Figure 3: **The χ^2/dof contours for (left) all RHIC, (middle) PHENIX only, and (right) fixed-target only.**

Energy Dependence Strongly Affected by Fit Results

Need to include STAR point to get good agreement with PHENIX result

Outer bands show the effect of including even most extreme values (like $(m, \mu_F/m, \mu_R/m) = (1.5, 0.5, 2)$ and $(1.5, 2, 0.5)$ for FONLL), difference negligible

Excluding RHIC results does not affect fixed-target region but broadens and softens energy dependence for $\sqrt{s} > 100$ GeV

Similar results found for higher masses, energy dependence less steep

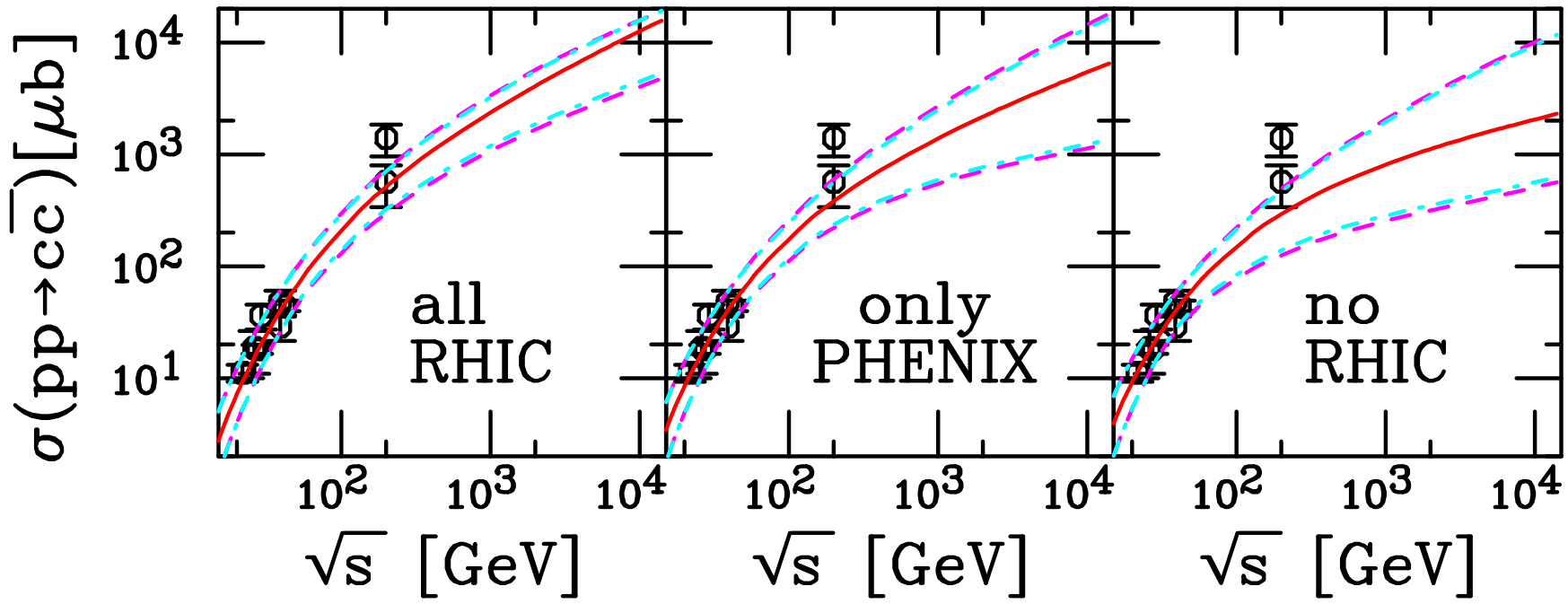

Figure 4: **The energy dependence of the charm total cross section compared to data with the central value and the uncertainty band found from the fits for (left) all RHIC, (middle) PHENIX only, and (right) fixed-target only.**

Effect on p_T Dependence

D meson semileptonic decays to electrons somewhat steeper at intermediate p_T

Agreement with PHENIX data not as good with narrower band; overall larger scale for charm gives steeper p_T dependence

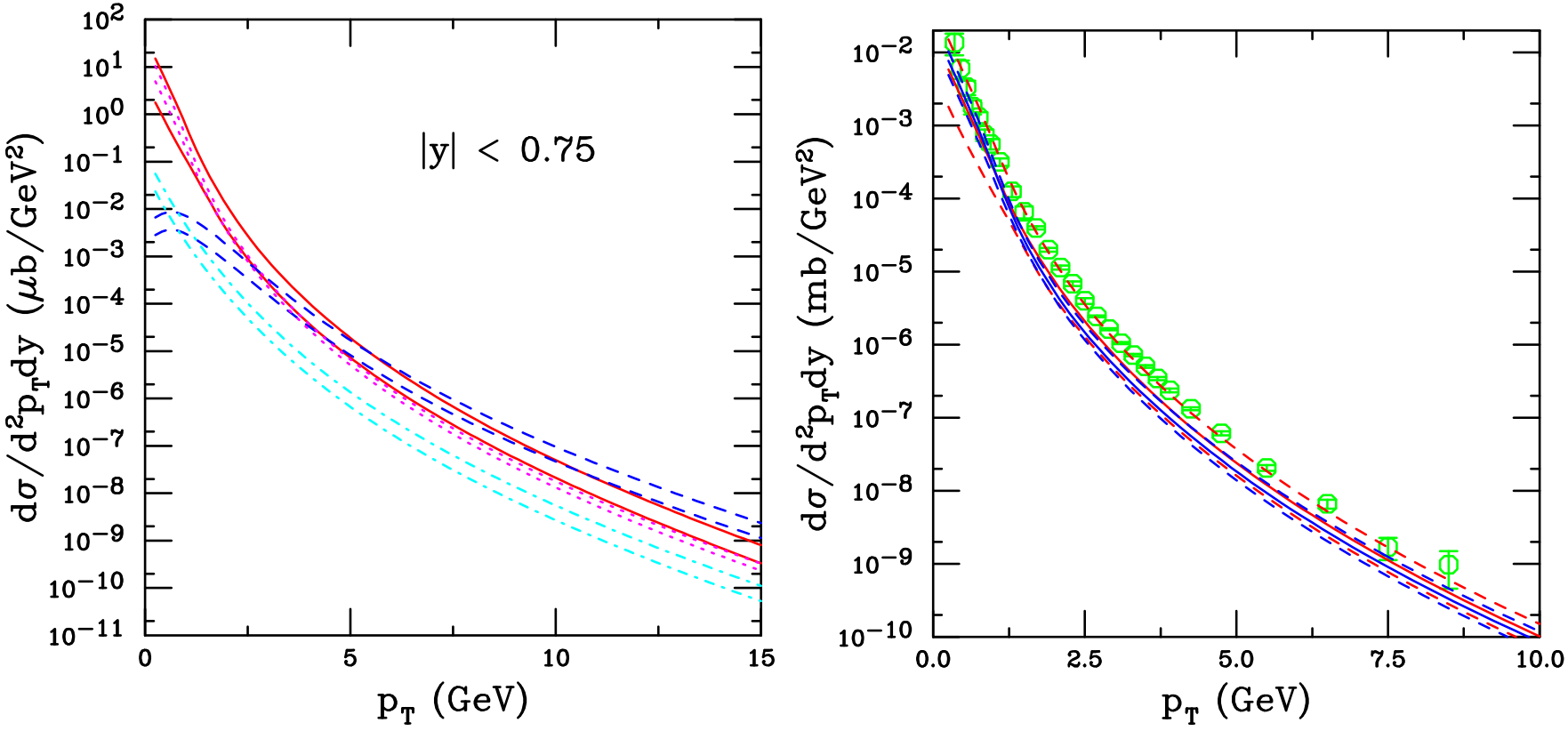

Figure 5: **(Left) The components of the electron spectrum: $B \to e$ (dashed blue); $B \to D \to e$ (dot-dashed cyan); $D \to e$ with the FONLL parameters (solid red) and around $m = 1.27$ GeV (dotted magenta). (Right) The sum of the contributions are compared with the FONLL set for charm (red) and $m = 1.27$ GeV (blue). The PHENIX data are also shown.**

Application to J/ψ: Color Evaporation

All quarkonium states are treated like $Q\overline{Q}$ ($Q = c, b$) below $H\overline{H}$ ($H = D, B$) threshold

Distributions for all quarkonium family members similar, modulo decay feed down, production ratios should be independent of $\sqrt{s}$

At LO, $gg \to Q\overline{Q}$ and $q\overline{q} \to Q\overline{Q}$; NLO add $gq \to Q\overline{Q}q$

$$\sigma_Q^{\rm CEM} = F_Q \sum_{i,j} \int_{4m_Q^2}^{4m_H^2} d\hat{s} \int dx_1 dx_2 \; f_{i/p}(x_1, \mu^2) \; f_{j/p}(x_2, \mu^2) \; \hat{\sigma}_{ij}(\hat{s}) \; \delta(\hat{s} - x_1 x_2 s)$$

Values of m_Q and Q^2 fixed from NLO calculation of $Q\overline{Q}$ production

Main uncertainties arise from choice of PDFs, heavy quark mass, renormalization (α_s) and factorization (evolution of PDFs) scales

Inclusive F_Q fixed by comparison of NLO calculation of $\sigma_Q^{\rm CEM}$ to $\sqrt{s}$ dependence of J/ψ and Υ cross sections, $\sigma(x_F > 0)$ and $Bd\sigma/dy|_{y=0}$ for J/ψ, $Bd\sigma/dy|_{y=0}$ for Υ

Data and branching ratios used to separate the F_Q's for each quarkonium state

Resonance	J/ψ	ψ'	χ_{c1}	χ_{c2}	Υ	Υ'	Υ''	$\chi_b(1P)$	$\chi_b(2P)$
$\sigma_i^{\rm dir}/\sigma_H$	**0.62**	**0.14**	**0.6**	**0.99**	**0.52**	**0.33**	**0.20**	**1.08**	**0.84**
f_i	**0.62**	**0.08**	**0.16**	**0.14**	**0.52**	**0.10**	**0.02**	**0.26**	**0.10**

Table 1: **The ratios of the direct quarkonium production cross sections, $\sigma_i^{\rm dir}$, to the inclusive J/ψ and Υ cross sections, denoted σ_H, and the feed down contributions of all states to the J/ψ and Υ cross sections, f_i, Digal *et al.*.**

Why Still CEM?

Open and hidden charm photo- and hadroproduction show similar energy dependence

High p_T Tevatron Run I data show that, within uncertainties of the data, the prompt J/ψ, the ψ' and χ_c p_T dependencies are the same

Amundsen *et al.* calculated p_T distribution (only partial real part) harder than data at high p_T, undershoots at low p_T – likely because they do not include any k_T smearing

Gavai *et al.* calculated complete J/ψ p_T distribution starting from exclusive NLO $Q\overline{Q}$ production code by Mangano *et al.*

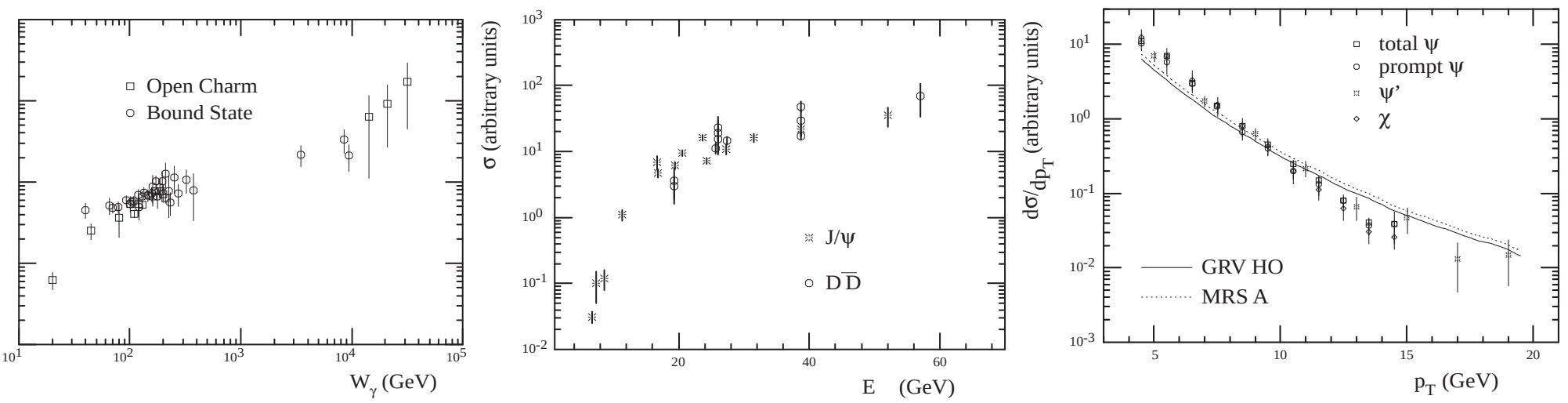

Figure 6: **(Left) Photoproduction data as a function of the photon energy in the hadron rest frame, W_γ. (Center) Hadroproduction data as a function of the center-of-mass energy, E_{cm}. In both cases, the normalization has been adjusted to show the similar shapes of the data. (Right) Run I data from the CDF Collaboration, shown with arbitrary normalization. The curves are the predictions of the color evaporation model at tree level, also shown with arbitrary normalization. [Amundson *et al.*]**

J/ψ Uncertainty with FONLL Parameter Set

Previously took 'by eye' fit to $Q\overline{Q}$ total cross section $(m, \mu_F/m, \mu_R/m) = (1.2, 2, 2)$

FONLL-based choice of parameters leads to upper limit only

Use fitted CEM parameter, F_C, at $(1.5, 1, 1)$ for all calculations in fiducial range

At large $\sqrt{s}$ $(\mu_F/m, \mu_R/m) = (0.5, 0.5)$, (0.5,1) flattens because $\mu_F < \mu_0$ of PDF

$m_c = 1.7$ GeV governs uncertainty at low $\sqrt{s}$: $m_D/m_c \sim 1.1$, small J/ψ phase space

Combination of large mass and scale uncertainty makes lower limit ill defined

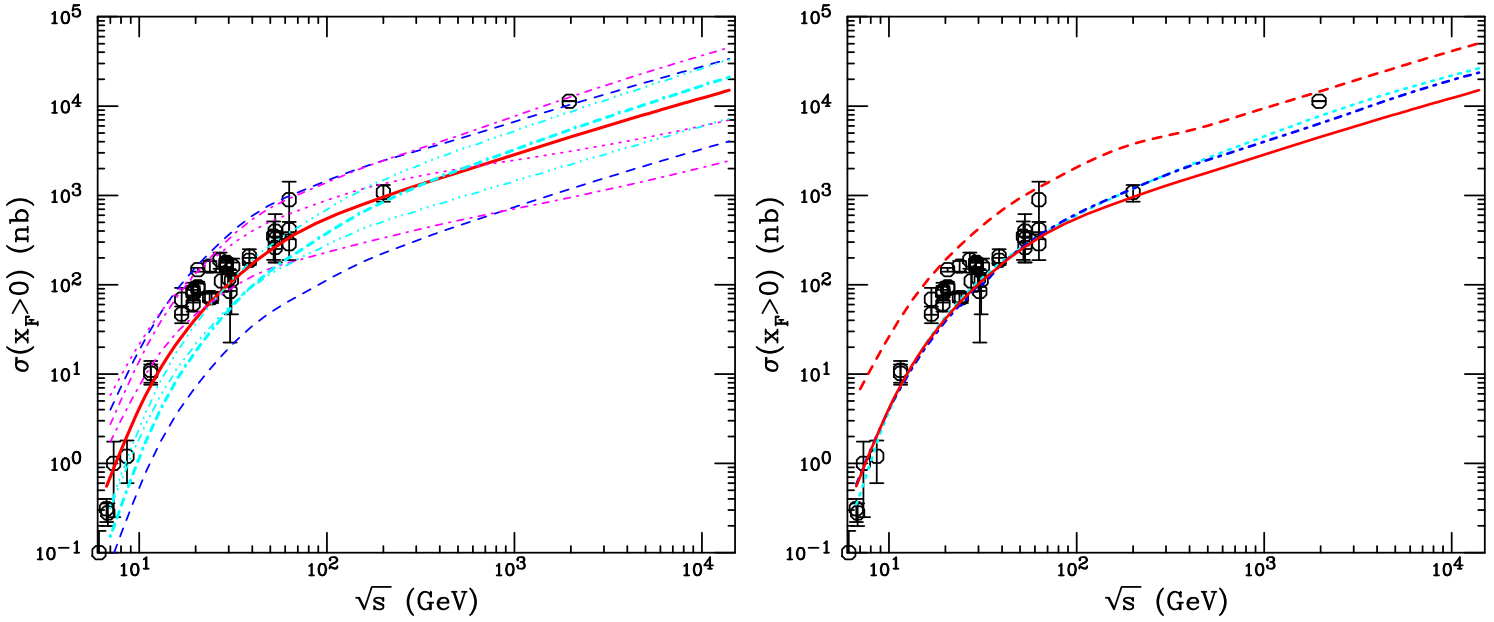

Figure 7: **(Left) Total J/ψ cross sections calculated using CTEQ6M. The solid red curve is the central value $(\mu_F/m, \mu_R/m) = (1, 1)$ with $m = 1.5$ GeV. The upper and lower dashed blue curves are $m = 1.3$ and 1.7 GeV with (1,1) respectively. The dotted magenta curve corresponds to (0.5,0.5) while the upper and lower magenta dot-dashed curves (above $\sqrt{s} = 50$ GeV) correspond to (1,0.5) and (0.5,1). The dash-dash-dotted cyan curve curresponds to (2,2) while the upper and lower cyan dot-dot-dot-dashed curves (above $\sqrt{s} = 50$ GeV) are (2,1) and (1,2). The last 6 curves are all calculated for $m_c = 1.5$ GeV. (Right) The solid and dashed red curves are the central value and upper limit for the J/ψ cross section. The solid cyan curve employs the MRST HO distributions while the dot-dashed blue curve is a result with CTEQ6M, both employing $m_c = 1.2$ GeV, $(\mu_F/m_T, \mu_R/m_T) = (2, 2)$.**

J/ψ Uncertainty with $m = 1.27$ GeV

Use fitted CEM parameter, F_C, at $(1.27, 2.8, 1.6)$ for all calculations in fiducial range

More phase space available for $c\bar{c}$ production below the $D\overline{D}$ threshold for the lower mass

Band describes J/ψ cross section data rather well, including CDF point

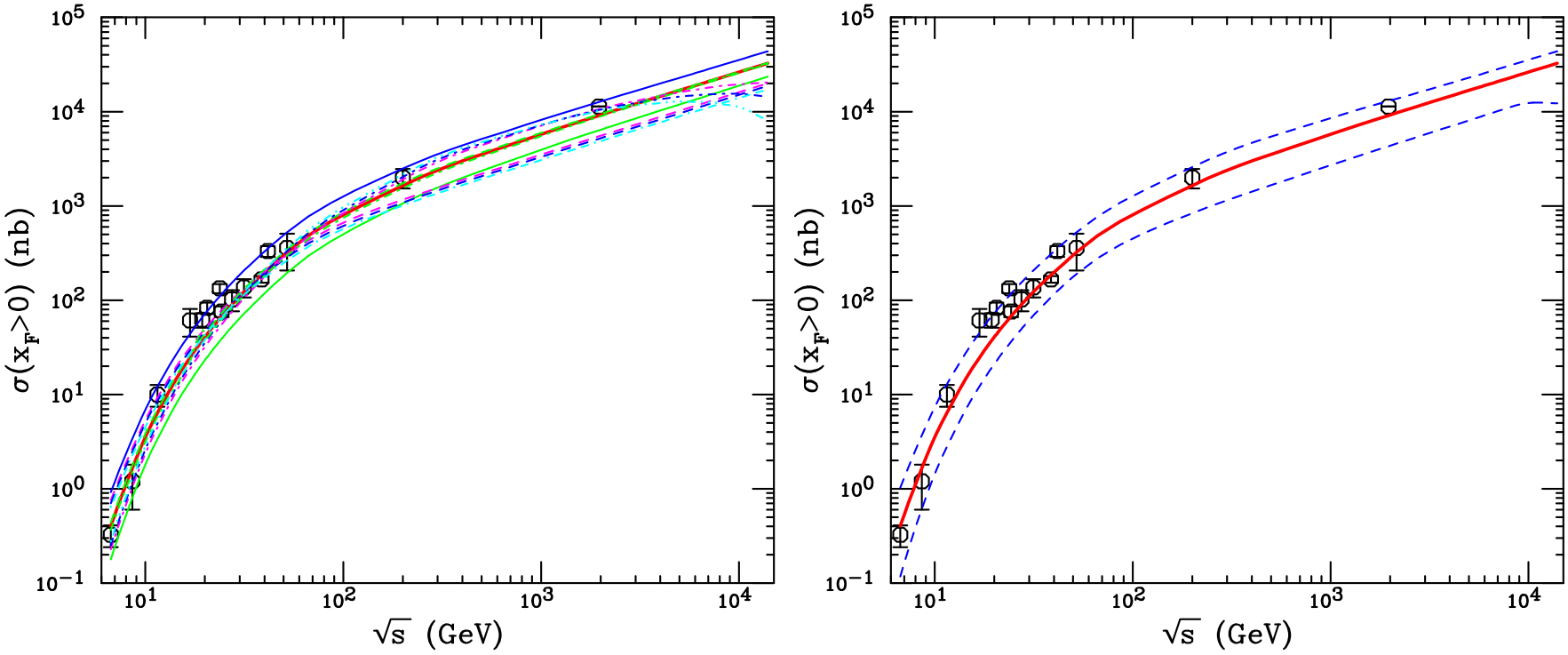

Figure 8: **(Left) Total J/ψ cross sections calculated using CTEQ6M. The solid red curve is the central value $(m, \mu_F/m, \mu_R/m) = (1.27, 2.8, 1.6)$ while the solid blue and green curves are calculated with $m = 1.18$ and 1.36 GeV respectively. The dashed magenta, blue and green curves correspond to $(1.27, 1.41, 1.49)$, $(1.27, 1.41, 1.6)$ and $(1.27, 1.41, 1.75)$ respectively while the dot-dashed magenta, blue and green curves are $(1.27, 5.91, 1.75)$, $(1.27, 5.91, 1.6)$ and $(1.27, 5.91, 1.49)$ respectively. (Right) The solid and dashed red curves are the central value and upper and lower limits for the J/ψ cross section.**

Comparison to RHIC pp J/ψ Data

Calculation reproduces shape of J/ψ p_T and y distributions rather well

No additional normalization factors are needed

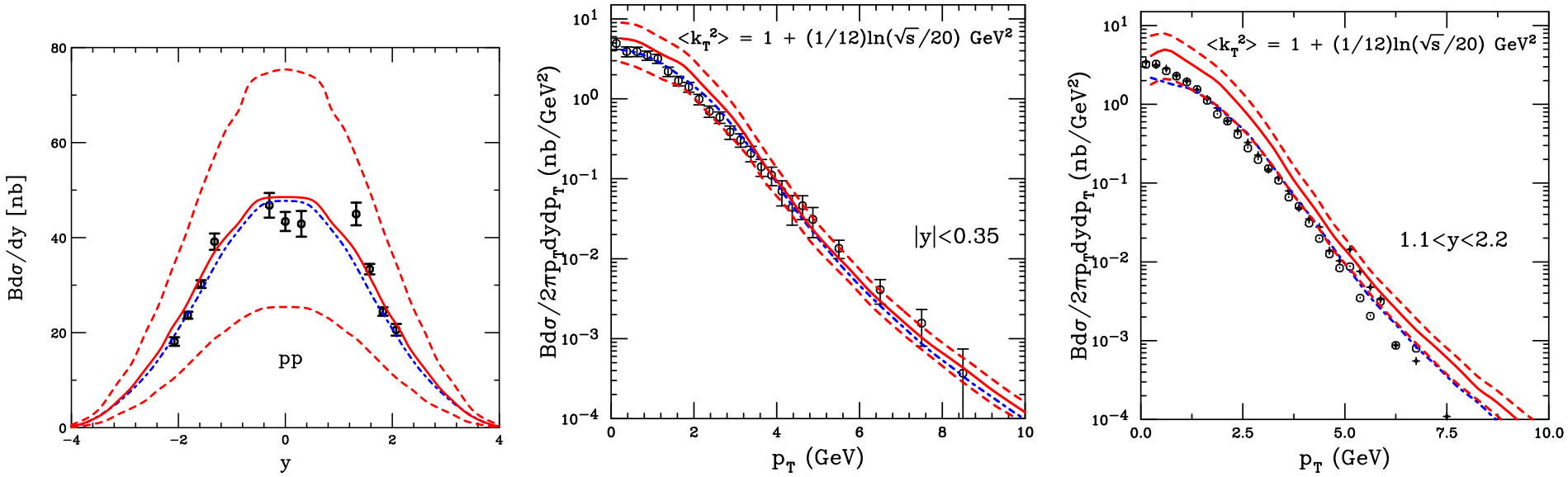

Figure 9: **PHENIX** pp **measurements compared to CEM calculation at** $\sqrt{s} = 200$ **GeV. The** J/ψ **rapidity distribution (left) and transverse momentum distributions at midrapidity (center) and in the muon arms (right). The band shows the results with** $m = 1.27$ **GeV, including the mass and scale uncertainties. Previous results, calculated with CTEQ6M and** $(m, \mu_F/m_T, \mu_R/m_T) = (1.2, 2, 2)$**, are shown as the dot-dashed curves. (The forward result in this case is scaled up by a factor of** ≈ 1.4**.) Both calculations employ** $\langle k_T^2 \rangle = 1.38$ **GeV**^{2}**.**

Calculation of 7 TeV pp J/ψ Distributions

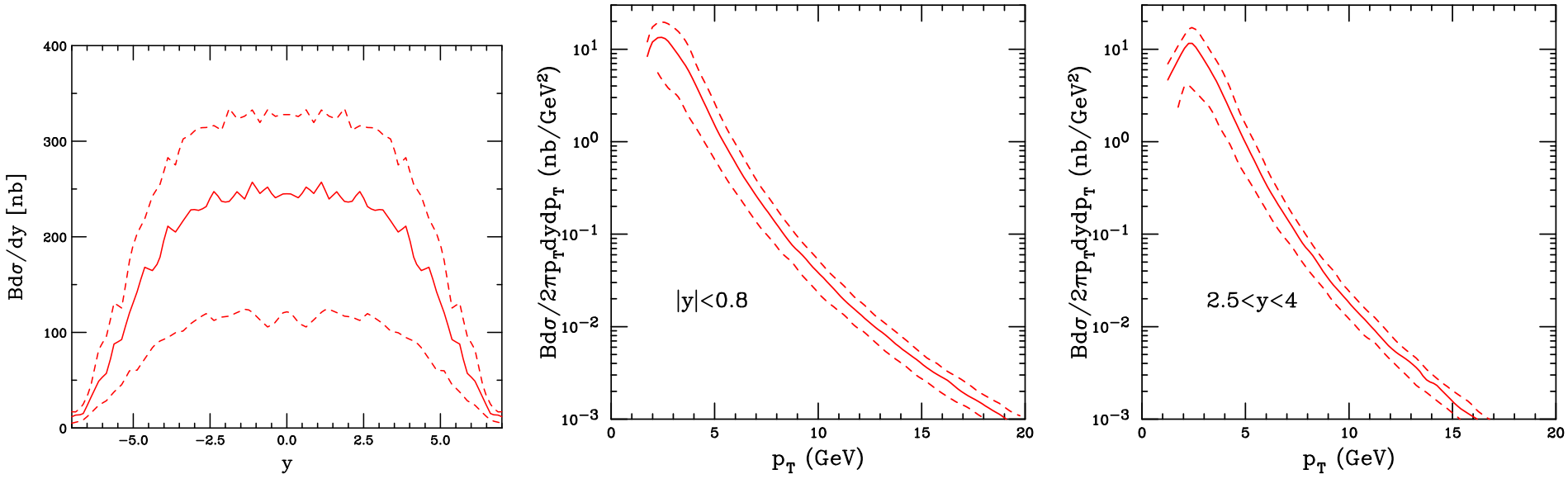

Figure 10: **Calculations of the J/ψ mid- and forward rapidity p_T distributions and y distributions at 7 TeV. The central value and the uncertainty bands are shown.**

Influence of Charm Mass and Scale on CNM at RHIC

Changing mass does not have a large effect on R_{dAu}, no absorption included here

Changing factorization scale from lower to higher values moves antishadowing peak closer to midrapidity while reducing peak size, due only to scale choice, not kinematics

Higher scale narrows uncertainty of EPS09 calculation, especially on lower limit
Renormalization scale effects cancel in ratio

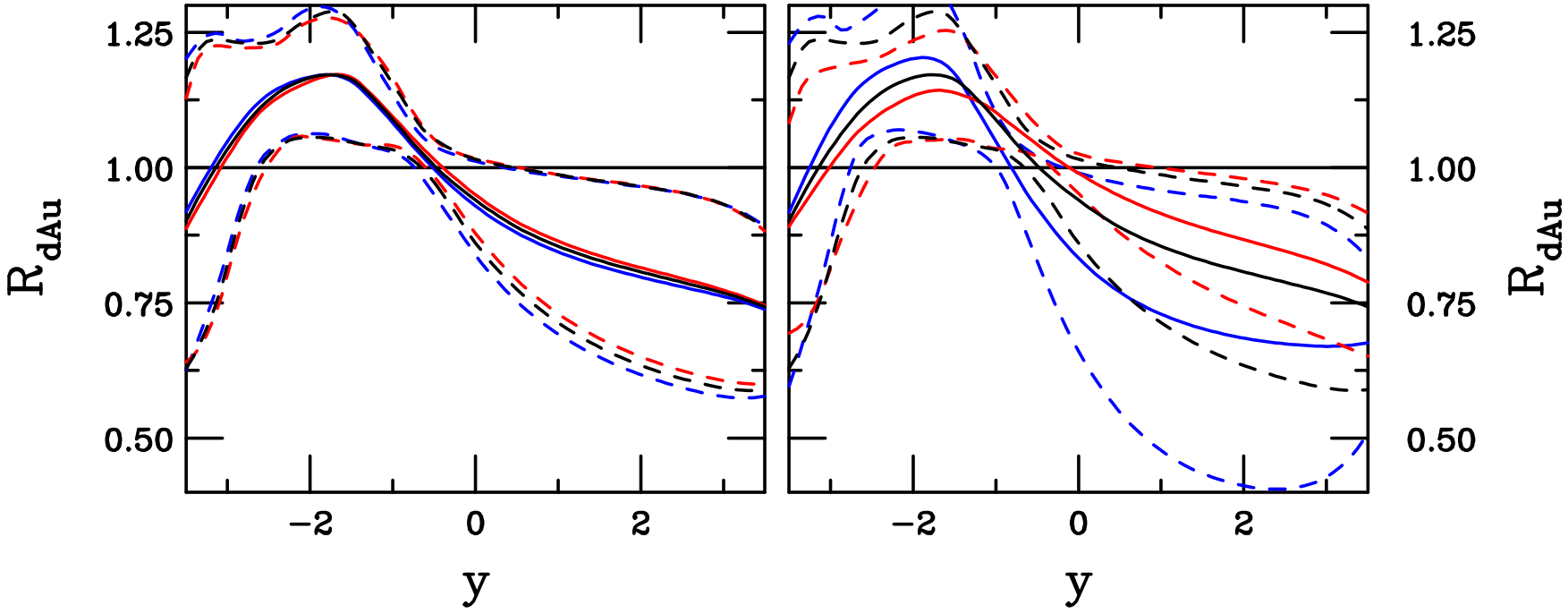

Figure 11: **The EPS09 uncertainty band in 200 GeV d+Au collisions at RHIC for (left) $m = 1.18$ (blue), 1.27 black, and 1.36 (red) GeV with the central scale values and for (right) $m = 1.27$ GeV with $\mu_F/m = 2.8$ (black), 1.41 (blue) and 5.91 (red).**

Influence of Charm Mass and Scale on CNM at LHC

$R_{p\mathrm{Pb}}$ shown at $\sqrt{s} = 2.76$ TeV, no absorption included

Similar effects seen at LHC as at RHIC, note different y-axis scales on the plots

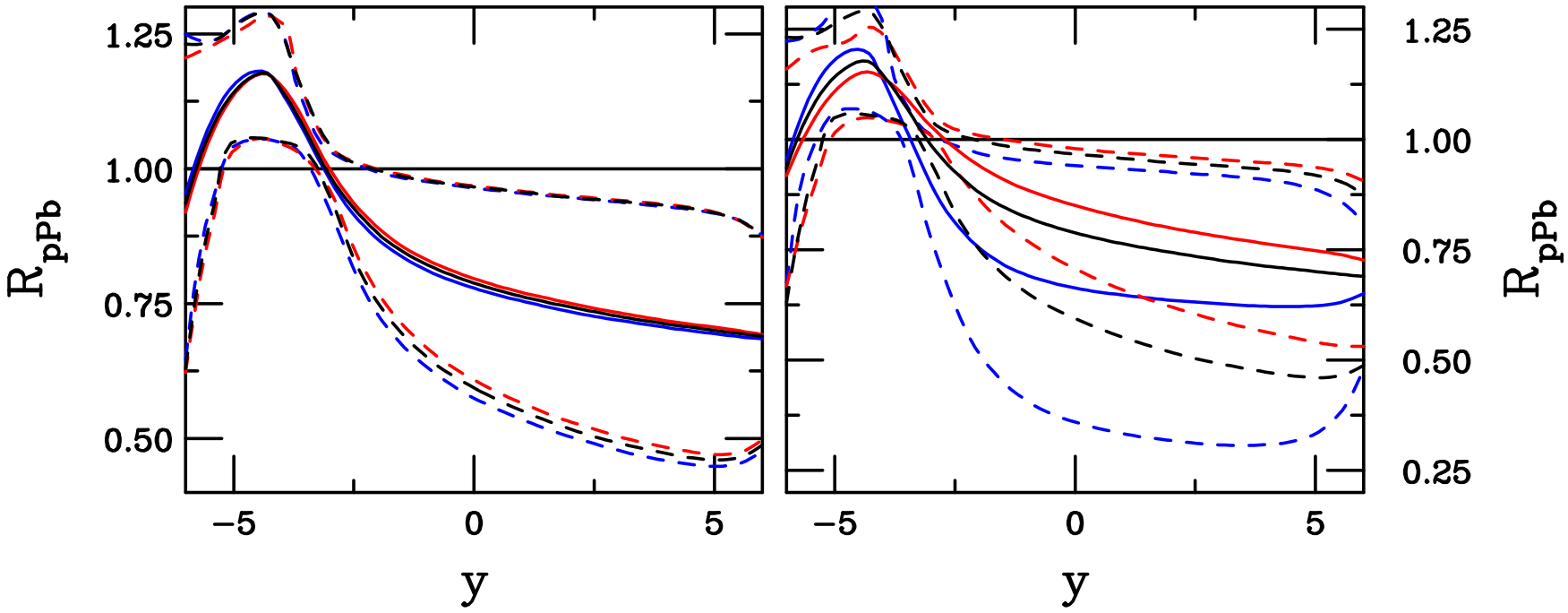

Figure 12: **The EPS09 uncertainty band in 2.76 TeV p+Pb collisions at the LHC for (left) $m = 1.18$ (blue), 1.27 black, and 1.36 (red) GeV with the central scale values and for (right) $m = 1.27$ GeV with $\mu_F/m = 2.8$ (black), 1.41 (blue) and 5.91 (red).**

Influence of Charm Mass and Scale on CNM in AA

Combined shadowing factors in AA collisions shows same trend, peaks shift depending on scale – move closer together for higher scales

Note that, in general, CNM effects are bigger for LHC (2.76 TeV, bottom) than at RHIC (200 GeV, top) so R_{AA} should be lower due to CNM alone

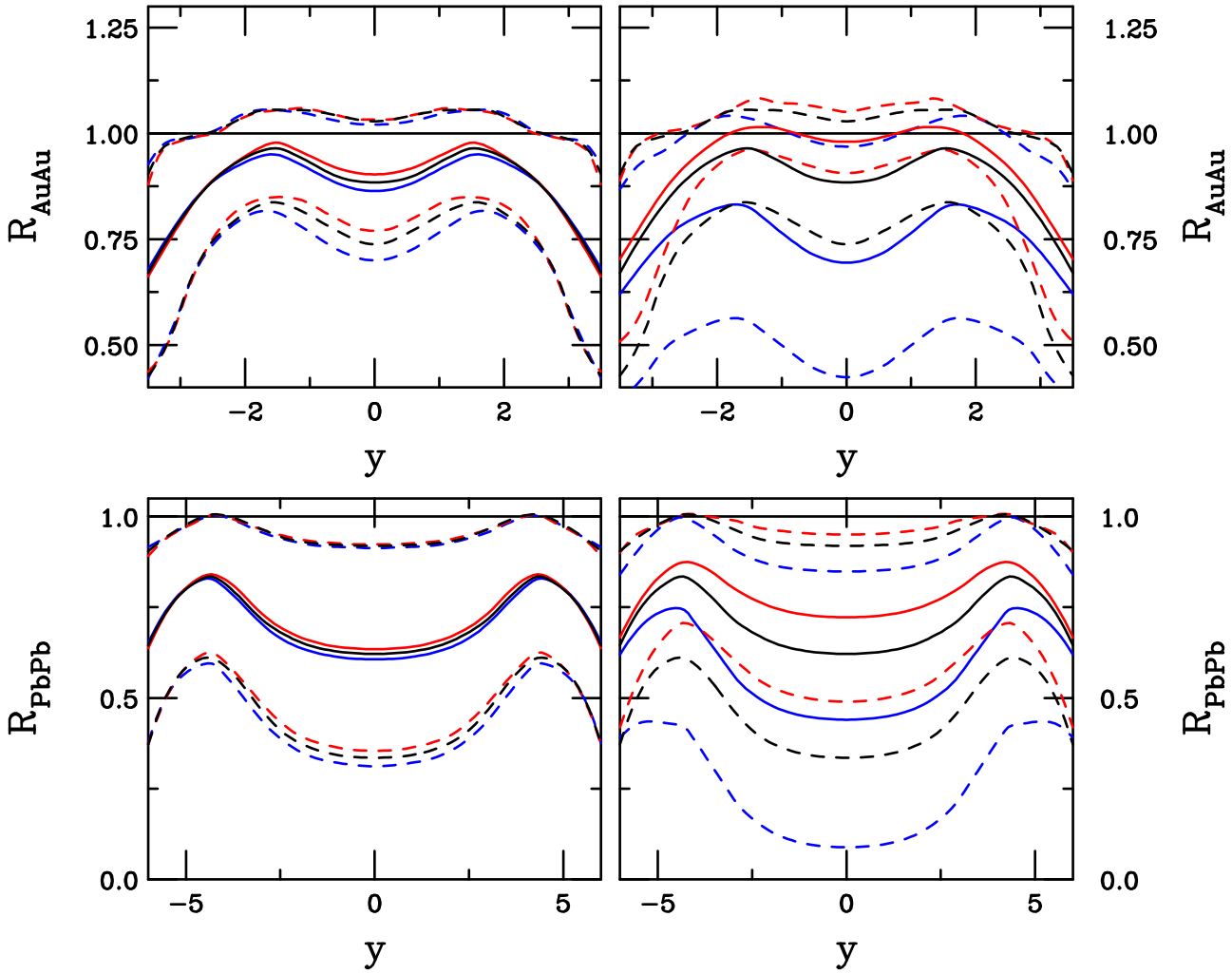

Figure 13: **The EPS09 uncertainty band in 200 GeV Au+Au collisions at RHIC (top) and 2.76 TeV Pb+Pb collisions at the LHC (bottom) for (left) $m = 1.18$ (blue), 1.27 black, and 1.36 (red) GeV with the central scale values and for (right) $m = 1.27$ GeV with $\mu_F/m = 2.8$ (black), 1.41 (blue) and 5.91 (red).**

Similar Suppression at SPS, RHIC and LHC?

If the suppression pattern in AA collisions over a wide range of energies is similar, it could be the ultimate CNM effect — due to production in the corona

Total J/ψ dissolution in the nuclear core region but survival in the corona would result in a universal suppression

Check the result in the hidden to open charm ratio if possible: all other cold matter effects would cancel (Satz, Digal, RV)

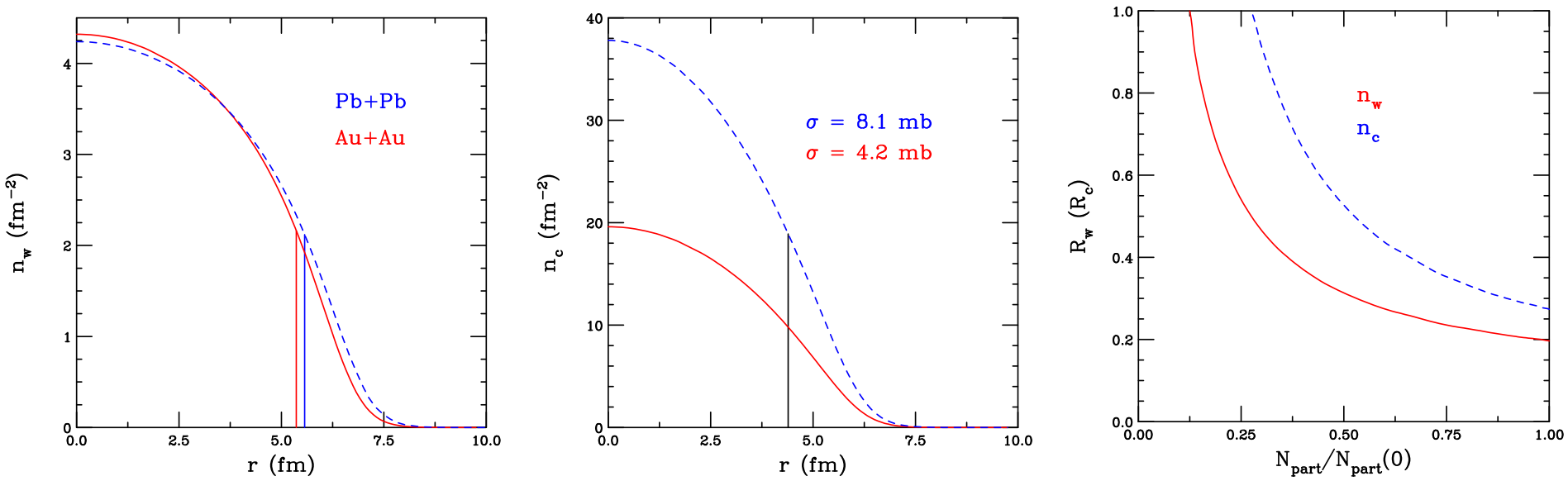

Figure 14: **The density of wounded nucleons, n_w, (left) and number of collisions, n_c, (center) as a function of transverse distance, r, at $b = 0$. The vertical bars indicate the distance at which the value of n_w or n_c respectively drops to half its value at $b = 0$. The two curves on the left hand side show the difference between n_w for Au+Au and Pb+Pb collisions while the two curves in the center highlight the fact that changing the NN cross section does not change the point where $n_c = n_c(b = 0)/2$. The right-hand plot shows the corona to core ratios for n_w and n_c (R_w and R_c respectively) as a function of the participant ratio, $N_{\rm part}/N_{\rm part}(b = 0)$.**

Summary

- Total charm cross sections have large theoretical uncertainties, primarily from scale choice and PDFs
- Uncertainty due to low x, low scale parton density is as large as those due to mass, scale and number of light flavors – can't be eliminated until more measurements in relevant region
- J/ψ uncertainty follows from charm uncertainty
- Scale choice alone plays a major role in the strength of cold matter effects on J/ψ production
- If J/ψ suppression is total in central nucleus-nucleus collisions, only observable production would be due to the cold corona